Carbenoxolone inhibits Pannexin1 channels through interactions in the first extracellular loop

Kevin Michalski and Toshimitsu Kawate

Department of Molecular Medicine, Field of Biochemistry, Molecular, and Cell Biology, Cornell University, Ithaca, NY 14853

Pannexin1 (Panx1) is an ATP release channel important for controlling immune responses and synaptic strength. Various stimuli including C-terminal cleavage, a high concentration of extracellular potassium, and voltage have been demonstrated to activate Panx1. However, it remains unclear how Panx1 senses and integrates such diverse stimuli to form an open channel. To provide a clue on the mechanism underlying Panx1 channel gating, we investigated the action mechanism of carbenoxolone (CBX), the most commonly used small molecule for attenuating Panx1 function triggered by a wide range of stimuli. Using a chimeric approach, we discovered that CBX reverses its action polarity and potentiates the voltage-gated channel activity of Panx1 when W74 in the first extracellular loop is mutated to a nonaromatic residue. A systematic mutagenesis study revealed that conserved residues in this loop also play important roles in CBX function, potentially by mediating CBX binding. We extended our experiments to other Panx1 inhibitors such as probenecid and ATP, which also potentiate the voltage-gated channel activity of a Panx1 mutant at position 74. Notably, probenecid alone can activate this mutant at a resting membrane potential. These data suggest that CBX and other inhibitors, including probenecid, attenuate Panx1 channel activity through modulation of the first extracellular loop. Our experiments are the first step toward identifying a previously unknown mode of CBX action, which provide insight into the role of the first extracellular loop in Panx1 channel gating.

The Journal of General Physiology

INTRODUCTION

Pannexin1 (Panx1) constitutes an ATP release channel that plays important roles throughout the body (Dahl and Keane, 2012; Penuela et al., 2014). In the immune system, for example, Panx1 mediates release of intracellular ATP as a "find-me" signal from apoptotic cells, facilitating the recruitment of macrophages for efficient cell clearance (Chekeni et al., 2010). In the nervous system, Panx1 controls synaptic excitability and plasticity (Thompson et al., 2008; Prochnow et al., 2012) and mediates propagation of astrocytic calcium waves (Thompson and Macvicar, 2008; Bernardinelli et al., 2011). Furthermore, recent studies using Panx1 knockout animals revealed that Panx1 contributes to noradrenergic vasoconstriction, which is important for blood pressure regulation (Billaud et al., 2015). Although the list of physiological and pathological roles of Panx1 has been rapidly extending, the mechanism of Panx1 channel opening remains poorly understood (Sandilos and Bayliss, 2012).

Interestingly, Panx1 can be activated by a remarkably wide range of stimuli. Panx1 channels open in response to activation of different membrane receptors (Locovei et al., 2006; Pelegrin and Surprenant, 2006; Thompson et al., 2008; Billaud et al., 2015), a high concentration of extracellular K^+ (Bao et al., 2004; Wang et al., 2014) or intracellular Ca^{2+} (Locovei et al., 2006), hypoxemia (Sridharan et al., 2010), caspase activation (Chekeni et al., 2010; Sandilos et al., 2012), and voltage stimulation (Bruzzone et al., 2003). How does Panx1 respond to such diverse stimuli? Functional Panx1 channels are most likely a hexamer (Boassa et al., 2007), where each subunit harbors four predicted transmembrane helices and intracellular N and C termini. One proposed Panx1 activation mechanism involves the C terminus, which has been shown to plug the transmembrane pore, rendering a resting Panx1 channel closed (Sandilos et al., 2012). Cleavage of this plug by caspase, in turn, opens the transmembrane pore. Although multiple studies support this mechanism (Dourado et al., 2014; Engelhardt et al., 2015), other gating mechanisms likely exist, as Panx1 channels truncated by ∼70 residues at the C terminus still remain closed at resting membrane potential (−60 mV) and open at a positive membrane potential (>20 mV; Jackson et al., 2014).

Regardless of the kind of activation stimulus, most previous studies, including those supporting the C-terminal plugging mechanism, demonstrate that Panx1 channel activity can be attenuated by application of a commonly used gap-junction blocker, carbenoxolone (CBX; Thompson et al., 2008; Chekeni et al., 2010; Sridharan

Correspondence to Toshimitsu Kawate: toshi.kawate@cornell.edu

Abbreviations used in this paper: CBX, carbenoxolone; CHO, Chinese hamster ovary; DIDS, 4,4′-diisothiocyano-2,2′-stilbenedisulfonic acid.

The Rockefeller University Press $30.00
J. Gen. Physiol. Vol. 147 No. 2 165–174
www.jgp.org/cgi/doi/10.1085/jgp.201511505

et al., 2010; Sandilos et al., 2012; Wang et al., 2014). We therefore rationalized that understanding how CBX inhibits Panx1 would be instrumental for dissecting the mechanism of how Panx1 channels open. This approach has been successfully used for dissecting the gating mechanisms of other ion channels, such as the *Shaker* K^+ channel (MacKinnon et al., 1988), the *drk1* K^+ channel (Swartz and MacKinnon, 1997a,b), and the TRPV1 channel (Bohlen et al., 2010). Here, we describe how CBX inhibits Panx1 opening using electrophysiology and mutagenesis of human Panx1 (hPanx1) expressed in HEK293 cells. We chose to use voltage as the Panx1 opening stimulus because it is a robust and commonly used stimulus for probing Panx1 channel function.

MATERIALS AND METHODS

Reagents

All chemicals were purchased from Sigma-Aldrich unless described otherwise.

Molecular biology

The full-length human Panx1 (Panx1; NCBI Protein GI: 39995064) and human Panx3 (Panx3; NCBI Protein GI: 16418453) genes were synthesized based on their protein sequences (GenScript) and cloned into the BamHI and XhoI sites of the pIE2 vector (modified from the pIRES-EGFP RK6 vector provided by M. Mayer, National Institutes of Health, Bethesda, MD) or a modified pIE2 vector containing an N-terminal flag tag. Point mutations were introduced into constructs via QuikChange site-directed mutagenesis (Agilent Technologies) or by PCR. The loop1 chimera construct was generated by PCR and contains residues 56–107 of Panx3. Chimera A contains residues 89–105 of Panx3, and chimera B contains residues 58–88 of Panx3. All chimeras and point mutations were generated based on the full-length Panx1 construct.

Electrophysiology

HEK293 cells were maintained in a humidified CO_2 incubator at 37°C in DMEM (Gibco) supplemented with 10% FBS (Atlanta Biologicals) and 10 µg/ml gentamicin (Gibco). 2 d before recording, cells were plated at a density of 10^5 cells/well onto 12-mm glass coverslips in wells of a 6-well plate (Corning). Cells were transfected with 300–800 ng plasmid DNA using FuGENE 6 (Promega) as per the manufacturer's instructions and used for electrophysiological recordings after 16–24 h. For recordings using Chinese hamster ovary (CHO) cells (CHO-K1; ATCC), cells were cultured in F-12K nutrient mix media (Gibco) supplemented with 10% FBS and 10 µg/ml gentamicin. Cells were plated to confluency on 35-mm dishes and transfected with 2 µg DNA using FuGENE 6 as directed by the manufacturer. Cells were trypsinized 24 h later, plated onto glass coverslips in wells of a 6-well plate, and used for electrophysiological recordings 2–6 h after plating. Borosilicate micropipettes (Harvard Apparatus) were pulled and heat polished to a final resistance of 1–6 MΩ and backfilled with pipette buffer containing (mM) 147 NaCl, 10 HEPES, and 10 EGTA, which was adjusted to pH 7.0 with NaOH. Whole cell patches were obtained in external buffer containing (mM) 147 NaCl, 2 KCl, 2 $CaCl_2$, 1 $MgCl_2$, 13 glucose, and 10 HEPES (adjusted to pH 7.3 with NaOH). Whole cell patches were perfused with external buffers with or without inhibitors using a rapid solution exchange system (RSC-200; Bio-Logic). Currents were recorded using an Axopatch 200B patch clamp amplifier (Axon Instruments), filtered at 2 kHz (Frequency Devices), digitized using Digidata 1440A (Axon Instruments) with a sampling frequency of 10 kHz, and analyzed using pCLAMP 10 software (Axon Instruments). To record pannexin channel activity, three similar voltage step protocols were used. In the first protocol, cells were held at −60 mV, stepped to a potential between −100 and 100 mV for 1 s (20 mV per step), and returned to −60 mV for 10 s to allow channels to close before the next step. In the second, which was used for current quantification (bar graphs and dose responses), cells were held at −50 mV, stepped to a potential between −100 and 100 mV for 0.5 s (50 mV per step), and returned to −50 mV for 2 s before the next step. In the third, used for conductance-voltage (G-V) plots, cells were held at −60 mV, stepped to a potential between −100 and 180 mV for 0.1 s (20 mV per step), and returned to −60 mV for 2 s. Because Panx1-expressing HEK293 cells sometimes exhibit leak currents that are relatively CBX insensitive even at negative potentials, we used the cells if the maximum current amplitude at 100 mV was at least 10-times greater than the current amplitude at −100 mV. Inhibitors of Panx1 were prepared fresh daily and used on the same day. Stock solutions of CBX (30 mM), ATP (1 M), and 4,4′-diisothiocyano-2,2′-stilbenedisulfonic acid (DIDS; 30 mM) were prepared in water and stock solutions of probenecid (300 mM) and glybenclamide (50 mM) were prepared in DMSO. All external solutions containing Panx1 inhibitors were adjusted to pH 7.3 with NaOH before application to cells.

Cell surface biotinylation

HEK293 cells were cultured as described in the previous section, plated in wells of a 6-well plate, and transfected at ∼80% confluency with 2 µg plasmid DNA (N-terminal flag tagged pannexins) using polyethylenimine (Polysciences). After 2-d incubation, cells were washed twice with PBS, transferred to a microcentrifuge tube, resuspended in 2 ml of 0.5 mg/ml sulfo-NHS-SS-biotin (Thermo Fisher Scientific), and rotated at 4°C for 40 min. Labeling was quenched by resuspending cells twice in PBS with 50 mM NH_4Cl for 5 min at 4°C, followed by two more washes with PBS. Cells were lysed by rotating for 30 min in RIPA buffer containing 150 mM NaCl, 3 mM $MgCl_2$, 1% NP-40, 0.5% deoxycholate (Anatrace), 0.1% SDS (Bio-Rad Laboratories), and 20 mM HEPES (adjusted to pH 7.4 with NaOH) and supplemented with protease inhibitor cocktail (Thermo Fisher Scientific). Lysates were cleared by centrifugation (22,000 *g*, 15 min), and equal amounts of protein were incubated with 35 µl streptavidin-Sepharose slurry (GE Healthcare; 50%; pre-equilibrated in RIPA buffer) for 2.5 h with inverting. Resin was washed six times with 700 µl RIPA buffer and eluted with SDS-PAGE sample buffer with 75 mM DTT (Thermo Fisher Scientific) for 30 min at 55°C with intermittent vortexing. Protein content was resolved using standard blotting techniques. In brief, protein was separated on 8% SDS-PAGE gels, blotted onto a PVDF membrane (Bio-Rad Laboratories), probed with monoclonal flag-M2 antibody (1:1,000) or monoclonal actin antibody (1:1,000; line AC-40), labeled with an anti–mouse AP-conjugate secondary antibody (1:1,000; Bio-Rad Laboratories), and developed using colorimetric AP substrate (Bio-Rad Laboratories).

Online supplemental material

Fig. S1 demonstrates that CBX modifies voltage-gated channel activity of Panx1 and the loop1 chimera expressed in CHO cells. Fig. S2 shows that WT-5S behaves similarly to the WT Panx1. Fig. S3 shows that DIDS attenuates Panx1-mediated channel activity almost irreversibly. Fig. S4 demonstrates that probenecid and CBX have no effect on untransfected HEK293 cells. Fig. S5 presents the effects of CBX and probenecid on the potassium-activated Panx1 currents. Online supplemental material is available at http://www.jgp.org/cgi/content/full/jgp.201511505/DC1.

RESULTS

A chimera between Panx1 and Panx3 reveals that the first extracellular loop plays a crucial role in CBX-mediated inhibition

The objective of this study was to dissect the action mechanism of CBX, a widely used small molecule for inhibiting Panx1 channel function. Because CBX can inhibit Panx1 channels activated by a variety of stimuli, understanding the action mechanism of CBX would help investigate the mechanism underlying Panx1 channel gating. To probe Panx1 channel activity, we performed whole cell voltage-clamp experiments using HEK239 cells transfected with Panx1. As reported previously (Bruzzone et al., 2003; Pelegrin and Surprenant, 2006; Ma et al., 2009), voltage stimuli gave rise to outwardly rectifying currents that were suppressed by extracellular CBX (Fig. 1 A). Notably, the extent of Panx1 current suppression by CBX was greater for strongly rectifying channels (∼90% suppression at 100 mV) than those weakly rectifying (∼50% suppression at 100 mV; Fig. 1 B), which was confirmed by a linear regression analysis (R = −0.75; Fig. 1 C). We therefore decided to use Panx1-expressing cells whose maximum current amplitude at 100 mV was at least 10-times greater than the current amplitude at −100 mV. We confirmed that the recorded channel activity was mediated by transfected Panx1, as untransfected cells exhibited little channel activity with or without CBX (Fig. 1, D and E).

To localize the important regions of Panx1 for CBX action, we took advantage of Panx3, a closely related Panx1 homologue that likely adopts a similar architecture to Panx1 (shares ∼45% sequence identity). Unlike Panx1, however, Panx3 does not give rise to current by voltage stimulation (Fig. 2 A, top) even though the surface expression in HEK293 cells was verified (Fig. 2 B, lanes "3"). Although the effect of CBX on Panx3 is unknown, it is possible that a Panx1/3 chimera, in which a domain of Panx1 important for CBX action is replaced with an equivalent domain of Panx3, may become insensitive to CBX. We generated a series of Panx1/3 chimeras and systematically analyzed the voltage-gated channel activity and the effect of CBX on each chimera. To our surprise, the voltage-gated channel activity of one of the chimeras, whose first extracellular loop of Panx1 was replaced with the equivalent loop of Panx3 (loop1 chimera), was actually enhanced by an application of CBX (Fig. 2 A, bottom). This result indicates that the action of CBX is likely mediated by the first extracellular loop. Although the mean current density of the loop1 chimera in the absence of CBX was about four times smaller than that of Panx1 (Fig. 2 C), this was not caused by a lower number of channels as this chimera expressed well on the cell surface (Fig. 2 B, lanes "C"). Also, the enhanced channel activity of the loop1 chimera by CBX was unlikely caused by unknown channels expressed in HEK293 cells, as we observed similar current enhancement from CHO cells transfected with the loop1 chimera (Fig. S1). Current enhancement of the loop1 chimera was dose dependent, and the

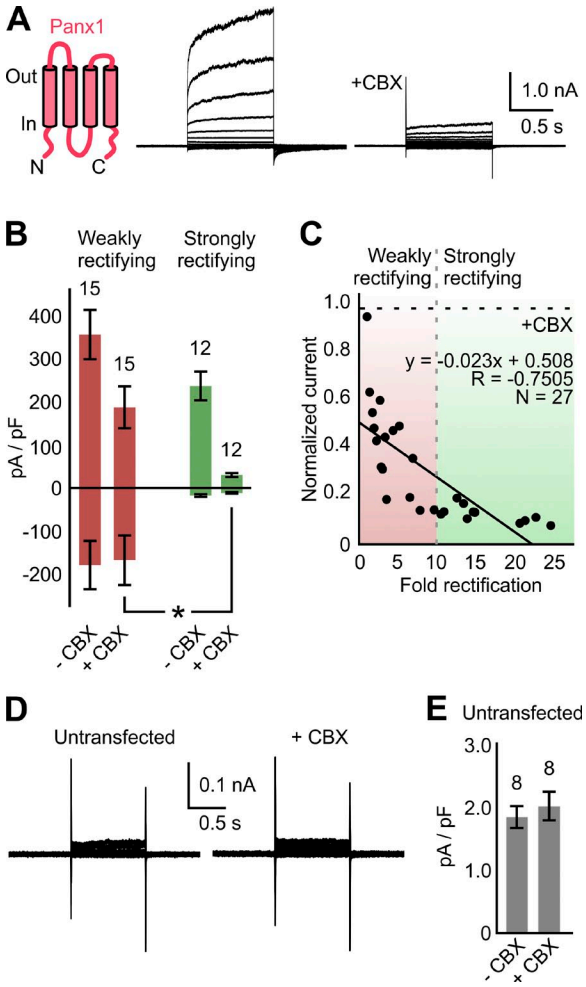

Figure 1. Voltage stimulations give rise to CBX-sensitive outward currents mediated by human Panx1 expressed in HEK293 cells. (A) Whole cell recordings of Panx1 in the absence (left) or presence (right) of 100 µM CBX. Voltages were stepped (−100 to 100 mV, 20-mV increments) from a holding potential of −60 mV. (B) Comparison of CBX sensitivity between Panx1-expressing HEK293 cells displaying weakly rectifying currents (red) and those displaying strongly rectifying currents (green). Bars represent mean current density at 100 and at −100 mV in the presence or absence of 100 µM CBX. Numbers above the graphs indicate the number of cells used for this experiment, and error bars represent SEM. Asterisks denote significance with $P < 0.05$ determined by Student's *t* test. (C) Linear regression analysis comparing current rectification with normalized current in the presence of 100 µM CBX. Each point represents a single cell used in B. (D) Whole cell recordings from an untransfected HEK293 cell in the absence (left) or presence (right) of 100 µM CBX. Cells were held at −60 mV and stepped between −100 and 100 mV (20-mV intervals). (E) Mean current density of untransfected HEK293 cells when stepped from a holding potential of −50 to 100 mV with or without 100 µM CBX. Bars represent mean current density of the indicated number of cells, and error bars represent SEM.

enhanced voltage-gated channel activity obtained with a saturating concentration of CBX (562 µM) was almost fourfold greater than that without CBX (Fig. 2 D).

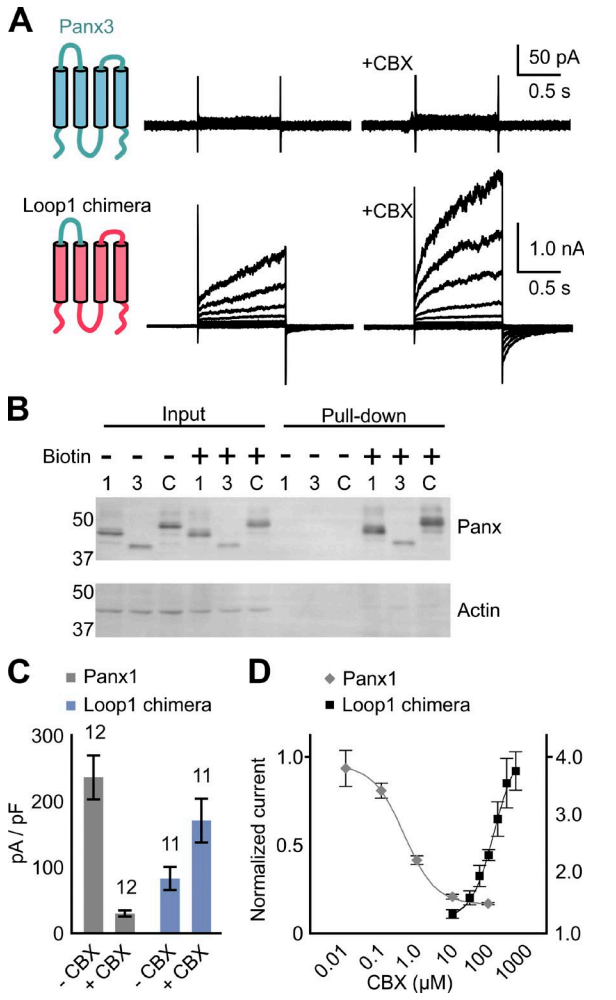

Figure 2. Inhibitory effect of CBX on voltage-activated Panx1 currents is reversed by swapping the first extracellular loop with Panx3. (A) Whole cell recordings of Panx3 (top) and the Panx1/3 loop1 chimera (bottom) in the absence (left) or presence (right) of 100 µM CBX. Voltages were stepped (−100 to 100 mV, 20-mV increments) from a holding potential of −60 mV. Loop1 chimera contains amino acids from the first extracellular loop of Panx3 (Q56 to L107). (B) Validation of cell surface–expressed Panx1, Panx3, and the loop1 chimera (1, 3, C, respectively). Each pannexin was tagged with an N-terminal flag peptide, and surface-expressed protein was labeled with sulfo-NHS-SS biotin. Labeled protein was enriched and analyzed by Western blots using anti-flag antibody (top). For loading and pull-down controls, Western blots using anti-actin antibody are also shown (bottom). Units are in kilodaltons. (C) Mean current densities of Panx1 (gray) and the loop1 chimera (blue). Voltages were stepped from −50 to 100 mV in the presence or absence of 100 µM CBX. Numbers above the bars indicate the number of cells used for this study, and error bars represent SEM. (D) CBX dose response of Panx1 (gray) and the loop1 chimera (black) activated by voltage stimuli (stepped from −50 to 100 mV). CBX-modified currents were normalized to the currents without CBX (left axis: Panx1; right axis: loop1 chimera). Each point represents the mean value of 5–12 cells, and error bars represent SEM.

These findings suggest that CBX is probably not a pore blocker, but likely a gating modulator that acts through the first extracellular loop of Panx1.

W74 plays central roles in CBX-mediated inhibition of Panx1

Among the 52 residues in the first extracellular loop, 26 residues are different between Panx1 and Panx3. Interestingly, the majority of different residues (15 out of 26) are clustered in the last 20 residues in this loop (Fig. 3). We wondered whether this variable region mediates CBX-dependent inhibition of Panx1 and whether substitution of this region with Panx3 confers the opposite effect of CBX on the loop1 chimera. To test this idea, we generated two variants of the loop1 chimera. The first chimera (chimera A) harbors the variable region of Panx3 but is otherwise Panx1 in this loop. The second chimera (chimera B) harbors the variable region of Panx1 but is otherwise Panx3 in this loop. Both chimeras responded well to voltage stimulation; however, chimera A was effectively inhibited by CBX (Fig. 4 A), which was against our idea that the variable region harbors important residues for CBX-mediated inhibition of Panx1. On the contrary, the voltage-gated channel activity of chimera B was enhanced by CBX, similar to what we observed with the parent loop1 chimera (Fig. 4 B). These results suggest that the relatively conserved region in the first extracellular loop harbors important residues for mediating CBX-dependent inhibition of Panx1.

To identify the residues important for CBX dependent inhibition of Panx1, we generated 11 single point mutants of Panx1, each of which contains a different Panx3 residue within the first ∼30 residues of the first extracellular loop. Among those, nine mutants were effectively inhibited by CBX, to an extent which WT Panx1 was inhibited (Fig. 4 C). In contrast, voltage-activated

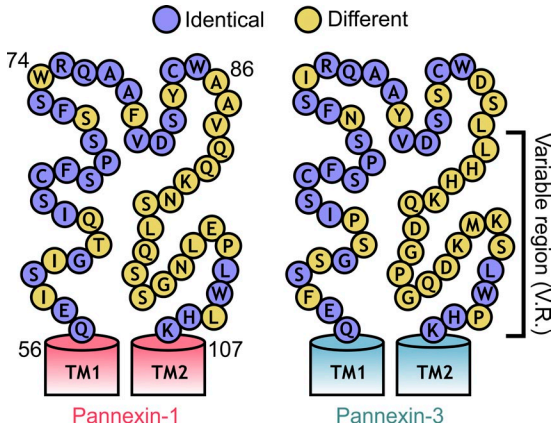

Figure 3. Sequence composition of the first extracellular loops of Panx1 and Panx3. Amino acids constituting the first extracellular loops of Panx1 (left; Q56 to K107) and Panx3 (right; Q56 to K108). Identical residues are colored in purple, and different residues are colored in yellow. The variable region (V.R.) is marked with a bracket.

currents of the W74I mutant were unchanged (or slightly enhanced), and that of the A86D mutant were inhibited only to 50% of its maximum (Fig. 4 C). Notably, CBX enhanced the voltage-activated current of W74I/A86D double mutant to a similar extent as this drug enhances the chimera B channel activity. Current densities of these mutants in the absence of CBX were comparable (Fig. 4 D). These data suggest that W74 and A86 in the first extracellular loop play important roles in CBX-mediated Panx1 inhibition. In particular, W74 seems to play a crucial role in determining the polarity of CBX action.

If W74 plays a key role in allowing CBX to function as an inhibitor, a single I74W mutation would convert loop1 chimera into a channel that is inhibited by CBX. Indeed, the voltage-activated current from the I74W loop1 chimera mutant was inhibited by 100 µM CBX (Fig. 5 A), a concentration that would enhance the

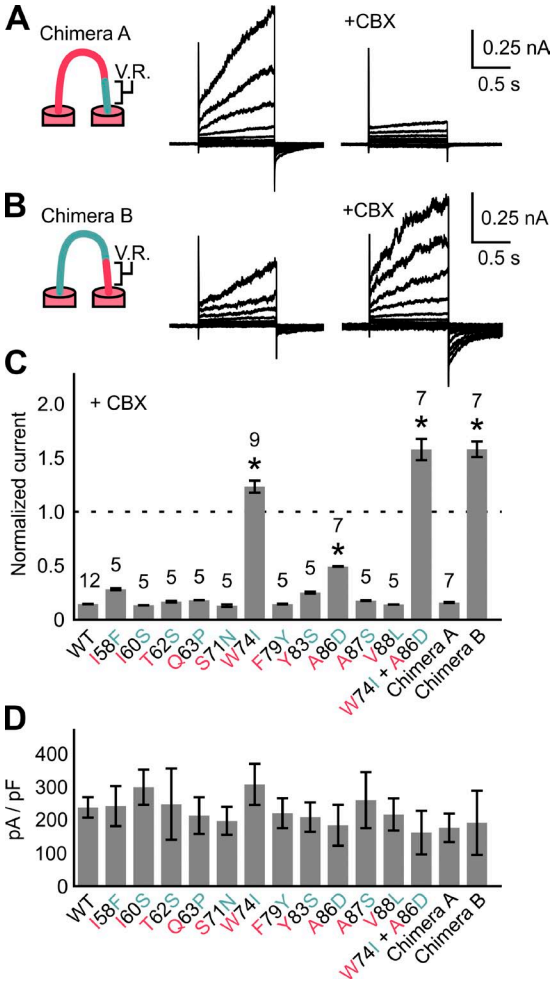

Figure 4. W74 in the first extracellular loop plays a central role in determining the polarity of CBX action. (A and B) Whole cell recordings of chimeras A and B in the absence (left) or presence (right) of 100 µM CBX. Voltages were stepped (−100 to 100 mV in 20-mV increments) from a holding potential of −60 mV. Chimera A harbors the variable region of Panx3, and chimera B harbors the other part of Panx3 in the first extracellular loop. (C) Panx1 point mutants were generated based on their Panx3 counterparts and tested for CBX-mediated current modification using the whole cell patch clamp method. Bars represent mean currents at 100 mV in the presence of 100 µM CBX normalized to the currents obtained in the absence of CBX. Error bars represent SEM of the indicated number of patches. Asterisks indicate significance of $P < 0.05$ determined by one-way ANOVA followed by Dunnett's test comparing WT with each mutant. Numbers above the bars indicate the number of cells used for this study. (D) Current densities of Panx1 mutants. Each bar represents mean current density at 100 mV, and error bars represent SEM.

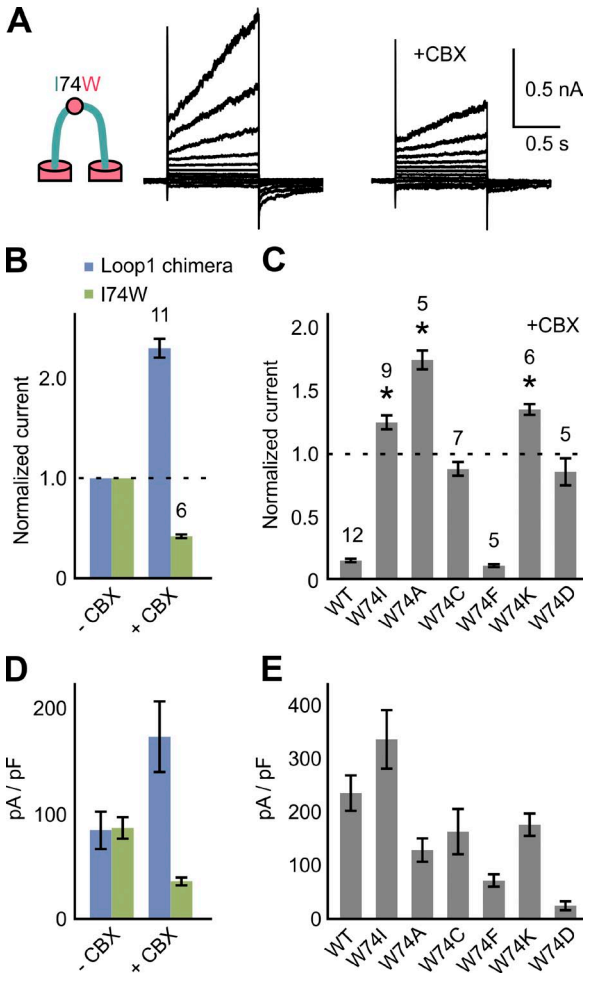

Figure 5. Amino acid at position 74 heavily influences the polarity of CBX action on voltage-activated Panx1 currents. (A) Whole cell patch clamp recordings presenting that the I74W mutation restores the inhibitory action of CBX on the loop1 chimera. Voltages were stepped (−100 to 100 mV with 20-mV increments) from the holding potential of −60 mV. (B) Normalized voltage-activated currents (100 mV) of the loop1 chimera (blue) and I74W mutant of the loop1 chimera (green). (C) Normalized CBX-modified currents of Panx1 mutants at position 74. Asterisks denote significant potentiation with $P < 0.05$ determined by one-sample Student's *t* test comparing each mutant with a value of 1.0. (D) Current densities of the loop1 chimera (blue) and the I74W mutant (green) at 100 mV in the absence (left) or presence (right) of 100 µM CBX. (E) Current densities of Panx1 mutants. Numbers above the bars indicate the number of cells used for these experiments. Each bar represents mean current density at 100 mV, and error bars represent SEM.

voltage-activated current of the loop1 chimera by ~2.3-fold (Fig. 5 B). This result strongly supports the idea that residue 74 in the first extracellular loop determines the polarity of CBX action and that tryptophan at this position enables CBX to function as an inhibitor. To further explore what kind of amino acid at position 74 possesses the ability to determine the polarity of CBX action, we created a series of single mutants at this position and compared the effect of CBX on voltage-gated channel activities. When W74 was mutated to alanine, we observed strong enhancement of the voltage-activated current (Fig. 5 C, W74A). When W74 was substituted with charged residues (i.e., Lys or Asp), CBX either weakly enhanced or only slightly inhibited the voltage-activated currents (Fig. 5 C, W74K and W74D). Likewise, when W74 was substituted with cysteine, CBX only slightly inhibited the voltage-activated current (Fig. 5 C, W74C). In contrast, when W74 was substituted with phenylalanine, CBX strongly inhibited the voltage-activated current (Fig. 5 C, W74F). The effect of CBX was unrelated to the current density of each mutant (Fig. 5, D and E). These results suggest that an aromatic amino acid at position 74 in the first extracellular loop mediates the inhibitory action of CBX, whereas other amino acids compromise or reverse this action.

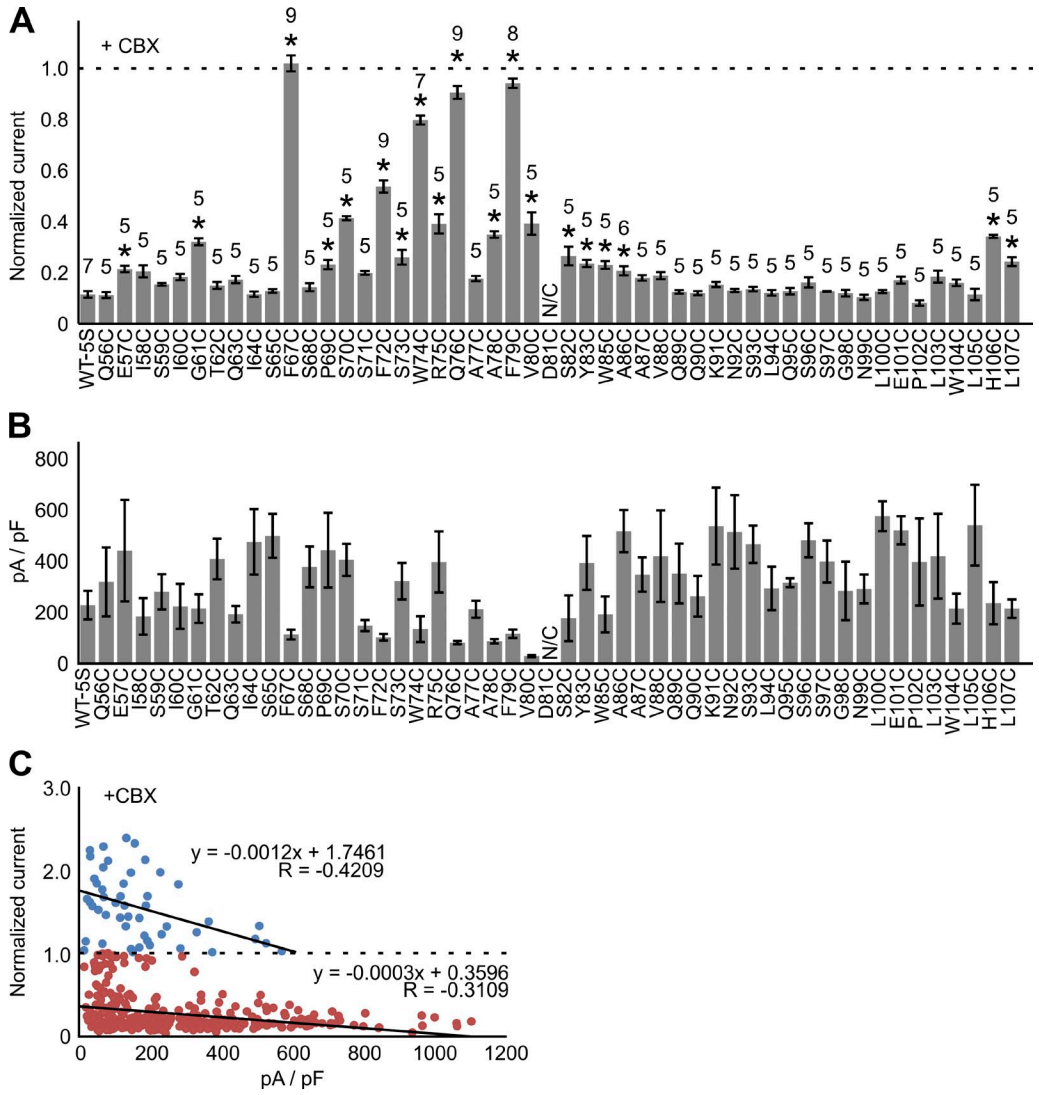

Figure 6. Point mutations in the first extracellular loop of Panx1 reveal potential residues that mediate CBX-dependent inhibition. (A) Quantification of whole cell currents triggered by voltage (100 mV) when treated with 100 µM CBX. Cysteine mutants were generated on a Panx1 construct where five internal cysteines were mutated to serine (WT-5S). Bars represent normalized mean currents, and error bars represent SEM. Numbers above the bars indicate the number of cells used for this study. Asterisks indicate significance with $P < 0.05$ determined by one-way ANOVA followed by Dunnett's test comparing WT-5S with each mutant. (B) Current densities of Cys mutants. Bars represent mean current density at 100 mV, and error bars represent SEM. N/C indicates no current. (C) Linear regression analyses comparing current density with normalized current in the presence of 100 µM CBX for all patches used in the present study ($n = 396$). Linear regression analyses were performed on cells that were potentiated upon CBX treatment (blue; $n = 49$) or patches that were inhibited by CBX (red; $n = 347$).

Several conserved residues between Panx1 and Panx3 also play important roles in CBX-dependent inhibition of Panx1

Thus far, we have focused on the different residues between Panx1 and Panx3 in the first extracellular loop, as these residues confer the enhancing activity of CBX on the loop1 chimera channel function. Given that CBX positively functions on the loop1 chimera, however, it is likely that the conserved residues between Panx1 and Panx3 also play roles in CBX action. For example, some of the conserved residues may mediate CBX binding. To systematically investigate the residues that contribute to CBX-dependent Panx1 inhibition, we generated cysteine mutants for all residues in this loop (residues 56–107) in Panx1 and examined the inhibitory action of CBX. To avoid potential disulfide formation between the introduced cysteine and naturally existing ones, we generated these cysteine mutants in "less cysteine" background, where five internal cysteines were mutated to serine (WT-5S: C136S, C170S, C216S, C347S, and C426S). Although a previous study suggests that the C426S mutation results in a constitutively open channel (Wang and Dahl, 2010), in our hands using HEK293 cells, WT-5S behaved similar to WT Panx1 (Fig. S2). We left C40 because a mutation at this position renders Panx1 channel constitutively open (Bunse et al., 2011). We also left C66 and C84 for their potential roles in forming a native disulfide bridge. Except for D81C, all cysteine mutants gave rise to voltage-dependent currents. When 100 µM CBX was included in the extracellular solution, currents from most mutants diminished to ∼10–20% of their maximum currents in a manner similar to WT-5S (Fig. 6 A). In contrast, currents from W74C, F67C, Q76C, and F79C remained mostly unchanged or only slightly reduced to ∼80% of their maximum currents. These results suggest that, besides the Panx1-specific W74, the conserved residues F67, Q76, and F79 also play important roles in CBX-mediated inhibition of Panx1. In this region (i.e., residues 67–86), the other mutants, except S68C, S71C, and A77C, presented mild but statistically significant resistance to CBX (currents reduced to ∼30–40%), suggesting that this region in the first extracellular loop plays central roles in the inhibitory action of CBX. Notably, A86C was inhibited by CBX to ∼25% of its maximum, suggesting that cysteine at this position mimics the role of alanine rather than aspartate. Altogether, these results suggest that conserved residues between Panx1 and Panx3 located between residues 67 and 86 in the first extracellular loop play crucial roles—mediating CBX binding, for example—in CBX-mediated inhibition of Panx1 channel activity.

We found no obvious correlation between the current density and CBX-normalized currents from these Cys mutants (Fig. 6 B). To analyze the relationship between the current density and CBX-normalized current in general, we plotted these values for all the cells that were treated with CBX ($n = 396$), divided into two groups (inhibited vs. potentiated by CBX), and performed a linear regression analysis for each group (Fig. 6 C). We found only a minor correlation for the cells that are inhibited by CBX ($R = -0.31$), where 100 pA/pF difference would change the effect of CBX only by ∼3%. This result disputes the idea that a moderate effect on inhibition could simply be caused by larger starting currents. Although we did observe a mild correlation between the current density and CBX-normalized current for the cells that are potentiated by CBX ($R = -0.42$), the correlation and the slope (100 pA/pF difference would change the effect of CBX by ∼10%) seem too weak to support the idea that activation by the drugs only happens in chimeras/mutants with small initial currents. Indeed, the channel activity of several constructs with >500 pA/pF current densities was enhanced by CBX.

Other Panx1 inhibitors also enhance the voltage-gated channel activity of the W74A mutant

We have demonstrated that a single residue at position 74 in the first extracellular loop can switch the polarity of CBX action on Panx1 channel activity, which strongly supports the idea that CBX functions as a gating modulator of Panx1. Do other Panx1 inhibitors function through a common modulation site? If they do, such Panx1 inhibitors may also enhance Panx1 channel activity when W74 is mutated to a nonaromatic residue. To test this idea, we compared voltage-activated currents of the W74A mutant with or without four different inhibitors, namely, glybenclamide (150 µM), ATP (10 mM), probenecid (3 mM), and disodium DIDS (200 µM). Because the EC_{50} of CBX on the loop1 chimera (∼120 µM; Fig. 2 D) was ∼40-times higher than the IC_{50} on Panx1

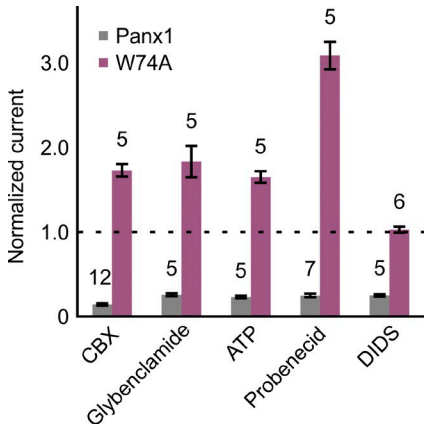

Figure 7. Several known Panx1 inhibitors also enhance voltage-activated currents of the Panx1 W74A point mutant. Bars represent mean currents in the presence of different inhibitors at 100 mV. Currents were normalized to those in the absence of inhibitors. Gray: Panx1; purple: Panx1 W74A. Concentrations used for each drug were as follows: 100 µM CBX, 150 µM glybenclamide, 10 mM ATP, 3 mM probenecid, and 200 µM DIDS. Numbers above the bars indicate the number of cells used for this study, and error bars represent SEM.

(∼2 µM; Fig. 2 D), we decided to use at least a 10-times higher concentration of each inhibitor than its published IC_{50} value (Ma et al., 2009; Qiu and Dahl, 2009), except for glybenclamide which was insoluble above a concentration ∼3-times higher than its IC_{50}. Among these four inhibitors, glybenclamide, ATP, and probenecid enhanced the voltage-activated channel activity of W74A (Fig. 7). In particular, probenecid enhanced the voltage-gated currents of W74A by ∼3-fold, which was even stronger than the effect of CBX (∼1.8-fold increase). DIDS, in contrast, did not alter the voltage-gated currents of W74A, suggesting that its mechanism of action may be different even though it also relies on residue 74 to inhibit Panx1. In support of this idea, the off rate of DIDS was substantially slower than those of the other inhibitors, making the reaction almost irreversible at a high concentration (Fig. S3). These results highlight that W74 is essential not only for CBX, but also for the other four Panx1 inhibitors to function. Furthermore, our results demonstrate that these inhibitors, except for DIDS, can positively modulate Panx1 through the first extracellular loop when tryptophan at 74 is mutated to alanine.

Probenecid can activate the W74A mutant without voltage stimulation

Given that the enhancing action of probenecid on the W74A mutant was remarkable (i.e., approximately threefold enhancement at 100 mV), we wondered whether probenecid alone could open W74A channels without voltage stimulation. When a cell expressing WT Panx1 was held at a resting membrane potential (−60 mV), probenecid did not give rise to inward currents, but instead, this drug attenuated the leak currents to some extent (Fig. 8 A, top traces). Interestingly, inhibition of the leak current was transient, and removal of probenecid gave rise to a large tail current, suggesting that binding of probenecid trapped Panx1 in a nonresting closed conformation. This effect of probenecid was not an off-target artifact, as this drug has no effect on untransfected HEK293 cells (Fig. S4). Though the exact mechanism is beyond the scope of this study, this result also supports the idea that probenecid functions as a gating modulator of Panx1. In contrast, both the loop1 chimera and the W74A mutant gave rise to inward currents upon probenecid application at −60 mV (Fig. 8 A, middle and bottom traces). These results indicate that probenecid can function as an agonist of Panx1 channel if the tryptophan residue is replaced with a nonaromatic residue at position 74 in the first extracellular loop. Though the loop1 chimera did give rise to a current at −60 mV in response to CBX application, the current amplitude was much weaker than that triggered by probenecid (Fig. 8 A, middle traces). To what extent do probenecid and CBX contribute to the enhanced currents of the W74A mutant at positive voltages? If these drugs open the W74A mutant channel independent of voltage stimulus, the G-V relationship would simply shift upward throughout the voltage range. In contrast, if these drugs work synergistically with voltage stimuli, the G-V curve would shift leftward. To examine how probenecid and CBX affect voltage-activated activity of the loop1 chimera, we analyzed the G-V relationship between −100 and 180 mV in the presence of probenecid or CBX. In both cases, the G-V curves exhibited a strong leftward shift and a weak upward shift (Fig. 8 B, closed red and black circles). Although the loop1 chimera in the absence of these drugs presented substantial voltage rectification (Fig. 8 B, gray circles), the large conductance at positive membrane potentials in the presence of these drugs cannot be explained as a simple addition of extra conductance equivalent to that observed at negative potentials. It is therefore likely that both probenecid and CBX potentiate voltage-gated channel activity of the loop1 chimera, supporting the idea that these drugs and voltage activate the loop1 chimera through a common gating mechanism.

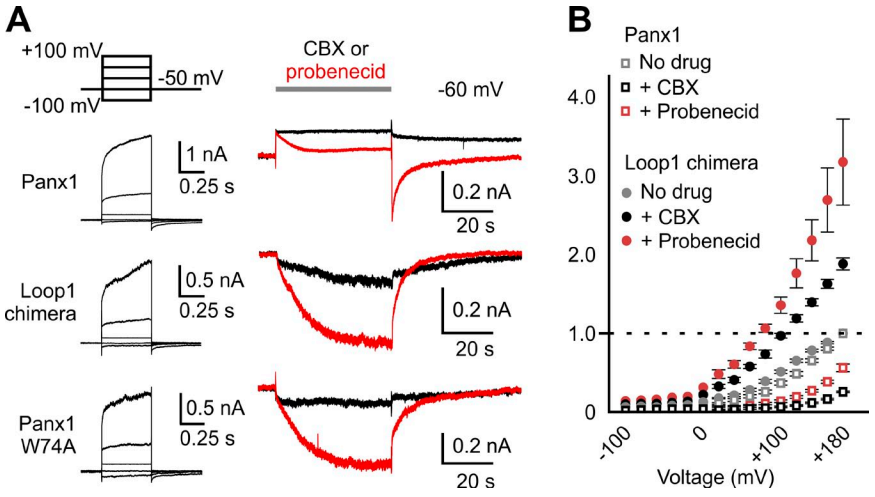

Figure 8. Probenecid can activate the Panx1 W74A point mutant at a resting membrane potential. (A) Whole cell recordings of Panx1 (top), loop1 chimera (middle), or W74A mutant (bottom) when exposed to 562 µM CBX (black) or 10 mM probenecid (red). Patches were held at −60 mV, and drugs were applied during the indicated length of time. Voltage-gated channel activity of each Panx1 construct is shown in the left traces. (B) G-V relationship of loop1 chimera (gray circles) and that in the presence of 100 µM CBX (black circles) or 3 mM probenecid (red circles). G-V relationship for WT Panx1 is shown as empty squares. Data were normalized to current without drugs at 180 mV. Each point represents the mean value, and error bars (shown only for points >0 mV) represent SEM ($n = 5–10$).

DISCUSSION

CBX has been widely used for inhibiting Panx1 and connexin gap junction channels; however, its mechanism of action remains unknown. In this study, we demonstrate that CBX inhibits Panx1 through modulation of the first extracellular loop, which likely plays a central role in Panx1 channel opening. Because a single mutation at position 74 in this loop does not merely abolish but actually reverses the inhibitory effect of CBX (Fig. 4), a simple pore-blocking mechanism is highly unlikely. Also, our cysteine-scanning mutagenesis experiments (Fig. 6) revealed that multiple residues in the first extracellular loop mediate CBX-dependent Panx1 inhibition, supporting the idea that CBX interacts with residues in this loop. Though one may argue that binding of CBX in the first extracellular loop might increase the unitary conductance or alter ion selectivity for voltage activation of the W74A mutant channel, such mechanisms cannot fully explain how CBX (and probenecid) opens this mutant channel in the absence of voltage stimulation (Fig. 8 A). Furthermore, the synergistic potentiative effect of CBX on the voltage-gated activity of the loop1 chimera supports that CBX binding facilitates channel opening of the loop1 chimera (Fig. 8 B). Therefore, modulation of Panx1 gating machinery is the likely mechanism of action for CBX.

Given that CBX has been successfully used to inhibit Panx1 channels activated by diverse stimuli, conformational changes in the first extracellular loop likely play an important role in Panx1 channel gating. This idea is supported by previous studies where chemical modifications of introduced cysteines in the first extracellular loop reduced voltage-gated Panx1 channel activity (Wang and Dahl, 2010). The fact that probenecid (and CBX to a lesser extent) can open the W74A mutant channel in the absence of voltage stimulation and that each drug potentiates (i.e., synergistically stimulates) the voltage-activated channel activity of this mutant, it is possible that movement of the first extracellular loop is coupled with Panx1 channel opening. We attempted to assess whether probenecid synergistically stimulates the loop1 chimera with a high concentration of potassium, another Panx1 activation stimulus that leads to a large conductance open state (Wang et al., 2014). Under our experimental condition, however, a high concentration of potassium (60 mM) gave rise to only a tiny current (<50 pA) such that the analysis of synergism was technically challenging (Fig. S5). Nevertheless, the loop1 chimera–mediated current was smaller than that of Panx1, suggesting that extracellular potassium may also act through the first extracellular loop. It would be interesting to investigate whether CBX potentiates the W74A mutant channel activity triggered by other stimuli, such as C-terminal cleavage by caspase and high concentration of intracellular calcium.

In this study, we used a chimeric approach to identify W74 as the central player for controlling the polarity of CBX action on Panx1 channel activity. The key discovery was that CBX actually potentiates, instead of simply not affecting, the voltage-gated channel activity of the loop1 chimera, which includes a W74A mutation. We therefore concluded that W74 actively drives the inhibitory action of CBX, whereas other residues support its function, possibly by mediating CBX binding. Indeed, our cysteine mutagenesis experiments demonstrate that most residues between 67 and 86 in the first extracellular loop play important roles in CBX-mediated inhibition of Panx1 (Fig. 6). Interestingly, 9 out of 19 residues in this region are hydrophobic residues that may directly mediate the binding of CBX, a glycyrrhetinic acid derivative harboring a steroid-like structure. Notably, previous studies also highlighted the importance of W74 in Panx1 inhibition mediated by several drugs, including ATP, probenecid, and CBX (to a lesser extent; Qiu et al., 2012; Wang et al., 2013). However, these studies showed diminished inhibitory effect of CBX on the W74A mutant but not the potentiative effect that we observed in our experiments. Although the exact reason for this discrepancy is unclear, the previous studies used *Xenopus laevis* oocytes where Panx1 channel properties may be affected by cytosolic components or different membrane components.

In conclusion, our current study provides a much needed first clue for how CBX inhibits Panx1 channels. Although our study does not exclude a possibility that other parts of Panx1 may contribute to the action of CBX, the first extracellular loop seems to play a central role in CBX-mediated Panx1 channel inhibition. We expect that further investigations focusing on the movement and regulation of the first extracellular loop will provide valuable insights into the mechanism underlying Panx1 channel gating.

We thank the members of the Kawate laboratory for discussions.

This work was supported by the National Institutes of Health (grant GM114379 to T. Kawate and grants GM008267 and GM007273 to K. Michalski).

The authors declare no competing financial interests.

Angus C. Nairn served as editor.

Submitted: 28 August 2015
Accepted: 18 December 2015

REFERENCES

Bao, L., S. Locovei, and G. Dahl. 2004. Pannexin membrane channels are mechanosensitive conduits for ATP. *FEBS Lett.* 572:65–68. http://dx.doi.org/10.1016/j.febslet.2004.07.009

Bernardinelli, Y., C. Salmon, E.V. Jones, W.T. Farmer, D. Stellwagen, and K.K. Murai. 2011. Astrocytes display complex and localized calcium responses to single-neuron stimulation in the hippocampus. *J. Neurosci.* 31:8905–8919. http://dx.doi.org/10.1523/JNEUROSCI.6341-10.2011

Billaud, M., Y.H. Chiu, A.W. Lohman, T. Parpaite, J.T. Butcher, S.M. Mutchler, L.J. DeLalio, M.V. Artamonov, J.K. Sandilos,

A.K. Best, et al. 2015. A molecular signature in the pannexin1 intracellular loop confers channel activation by the α1 adrenoreceptor in smooth muscle cells. *Sci. Signal.* 8:ra17. http://dx.doi.org/10.1126/scisignal.2005824

Boassa, D., C. Ambrosi, F. Qiu, G. Dahl, G. Gaietta, and G. Sosinsky. 2007. Pannexin1 channels contain a glycosylation site that targets the hexamer to the plasma membrane. *J. Biol. Chem.* 282:31733–31743. http://dx.doi.org/10.1074/jbc.M702422200

Bohlen, C.J., A. Priel, S. Zhou, D. King, J. Siemens, and D. Julius. 2010. A bivalent tarantula toxin activates the capsaicin receptor, TRPV1, by targeting the outer pore domain. *Cell.* 141:834–845. http://dx.doi.org/10.1016/j.cell.2010.03.052

Bruzzone, R., S.G. Hormuzdi, M.T. Barbe, A. Herb, and H. Monyer. 2003. Pannexins, a family of gap junction proteins expressed in brain. *Proc. Natl. Acad. Sci. USA.* 100:13644–13649. http://dx.doi.org/10.1073/pnas.2233464100

Bunse, S., M. Schmidt, S. Hoffmann, K. Engelhardt, G. Zoidl, and R. Dermietzel. 2011. Single cysteines in the extracellular and transmembrane regions modulate pannexin 1 channel function. *J. Membr. Biol.* 244:21–33. http://dx.doi.org/10.1007/s00232-011-9393-3

Chekeni, F.B., M.R. Elliott, J.K. Sandilos, S.F. Walk, J.M. Kinchen, E.R. Lazarowski, A.J. Armstrong, S. Penuela, D.W. Laird, G.S. Salvesen, et al. 2010. Pannexin 1 channels mediate 'find-me' signal release and membrane permeability during apoptosis. *Nature.* 467:863–867. http://dx.doi.org/10.1038/nature09413

Dahl, G., and R.W. Keane. 2012. Pannexin: from discovery to bedside in 11±4 years? *Brain Res.* 1487:150–159. http://dx.doi.org/10.1016/j.brainres.2012.04.058

Dourado, M., E. Wong, and D.H. Hackos. 2014. Pannexin-1 is blocked by its C-terminus through a delocalized non-specific interaction surface. *PLoS One.* 9:e99596. http://dx.doi.org/10.1371/journal.pone.0099596

Engelhardt, K., M. Schmidt, M. Tenbusch, and R. Dermietzel. 2015. Effects on channel properties and induction of cell death induced by C-terminal truncations of pannexin1 depend on domain length. *J. Membr. Biol.* 248:285–294. http://dx.doi.org/10.1007/s00232-014-9767-4

Jackson, D.G., J. Wang, R.W. Keane, E. Scemes, and G. Dahl. 2014. ATP and potassium ions: a deadly combination for astrocytes. *Sci. Rep.* 4:4576. http://dx.doi.org/10.1038/srep04576

Locovei, S., J. Wang, and G. Dahl. 2006. Activation of pannexin 1 channels by ATP through P2Y receptors and by cytoplasmic calcium. *FEBS Lett.* 580:239–244. http://dx.doi.org/10.1016/j.febslet.2005.12.004

Ma, W., H. Hui, P. Pelegrin, and A. Surprenant. 2009. Pharmacological characterization of pannexin-1 currents expressed in mammalian cells. *J. Pharmacol. Exp. Ther.* 328:409–418. http://dx.doi.org/10.1124/jpet.108.146365

MacKinnon, R., P.H. Reinhart, and M.M. White. 1988. Charybdotoxin block of Shaker K^+ channels suggests that different types of K^+ channels share common structural features. *Neuron.* 1:997–1001. http://dx.doi.org/10.1016/0896-6273(88)90156-0

Pelegrin, P., and A. Surprenant. 2006. Pannexin-1 mediates large pore formation and interleukin-1β release by the ATP-gated $P2X_7$ receptor. *EMBO J.* 25:5071–5082. http://dx.doi.org/10.1038/sj.emboj.7601378

Penuela, S., L. Harland, J. Simek, and D.W. Laird. 2014. Pannexin channels and their links to human disease. *Biochem. J.* 461:371–381. http://dx.doi.org/10.1042/BJ20140447

Prochnow, N., A. Abdulazim, S. Kurtenbach, V. Wildförster, G. Dvoriantchikova, J. Hanske, E. Petrasch-Parwez, V.I. Shestopalov, R. Dermietzel, D. Manahan-Vaughan, and G. Zoidl. 2012. Pannexin1 stabilizes synaptic plasticity and is needed for learning. *PLoS One.* 7:e51767. (published erratum appears in *PLoS One.* 2013. 8:http://dx.doi.org/10.1371/annotation/d0972416-5fef-4f89-9c09-cb4cb0c6295d) http://dx.doi.org/10.1371/journal.pone.0051767

Qiu, F., and G. Dahl. 2009. A permeant regulating its permeation pore: inhibition of pannexin 1 channels by ATP. *Am. J. Physiol. Cell Physiol.* 296:C250–C255. http://dx.doi.org/10.1152/ajpcell.00433.2008

Qiu, F., J. Wang, and G. Dahl. 2012. Alanine substitution scanning of pannexin1 reveals amino acid residues mediating ATP sensitivity. *Purinergic Signal.* 8:81–90. http://dx.doi.org/10.1007/s11302-011-9263-6

Sandilos, J.K., and D.A. Bayliss. 2012. Physiological mechanisms for the modulation of pannexin 1 channel activity. *J. Physiol.* 590:6257–6266. http://dx.doi.org/10.1113/jphysiol.2012.240911

Sandilos, J.K., Y.H. Chiu, F.B. Chekeni, A.J. Armstrong, S.F. Walk, K.S. Ravichandran, and D.A. Bayliss. 2012. Pannexin 1, an ATP release channel, is activated by caspase cleavage of its pore-associated C-terminal autoinhibitory region. *J. Biol. Chem.* 287:11303–11311. http://dx.doi.org/10.1074/jbc.M111.323378

Sridharan, M., S.P. Adderley, E.A. Bowles, T.M. Egan, A.H. Stephenson, M.L. Ellsworth, and R.S. Sprague. 2010. Pannexin 1 is the conduit for low oxygen tension-induced ATP release from human erythrocytes. *Am. J. Physiol. Heart Circ. Physiol.* 299:H1146–H1152. http://dx.doi.org/10.1152/ajpheart.00301.2010

Swartz, K.J., and R. MacKinnon. 1997a. Hanatoxin modifies the gating of a voltage-dependent K^+ channel through multiple binding sites. *Neuron.* 18:665–673. http://dx.doi.org/10.1016/S0896-6273(00)80306-2

Swartz, K.J., and R. MacKinnon. 1997b. Mapping the receptor site for hanatoxin, a gating modifier of voltage-dependent K^+ channels. *Neuron.* 18:675–682. http://dx.doi.org/10.1016/S0896-6273(00)80307-4

Thompson, R.J., and B.A. Macvicar. 2008. Connexin and pannexin hemichannels of neurons and astrocytes. *Channels (Austin).* 2:81–86. http://dx.doi.org/10.4161/chan.2.2.6003

Thompson, R.J., M.F. Jackson, M.E. Olah, R.L. Rungta, D.J. Hines, M.A. Beazely, J.F. MacDonald, and B.A. MacVicar. 2008. Activation of pannexin-1 hemichannels augments aberrant bursting in the hippocampus. *Science.* 322:1555–1559. http://dx.doi.org/10.1126/science.1165209

Wang, J., and G. Dahl. 2010. SCAM analysis of Panx1 suggests a peculiar pore structure. *J. Gen. Physiol.* 136:515–527. http://dx.doi.org/10.1085/jgp.201010440

Wang, J., D.G. Jackson, and G. Dahl. 2013. The food dye FD&C Blue No. 1 is a selective inhibitor of the ATP release channel Panx1. *J. Gen. Physiol.* 141:649–656. http://dx.doi.org/10.1085/jgp.201310966

Wang, J., C. Ambrosi, F. Qiu, D.G. Jackson, G. Sosinsky, and G. Dahl. 2014. The membrane protein Pannexin1 forms two open-channel conformations depending on the mode of activation. *Sci. Signal.* 7:ra69. http://dx.doi.org/10.1126/scisignal.2005431